

IMPACT OF SOIL SPATIAL VARIABILITY ON THE PERFORMANCE OF SUCTION CAISSONS IN SAND

Hongfen Zhao

School of Civil Engineering, Sun Yat-sen University, Zhuhai, China & State Key Laboratory for Tunnel Engineering, Sun Yat-Sen University, Guangzhou, China. E-mail: zhaohf7@mail.sysu.edu.cn.

JinBiao Mo

School of Civil Engineering, Sun Yat-Sen University, Guangzhou, PR China. E-mail: mojb@mail2.sysu.edu.cn

Haoyuan Liu

School of Transportation Science and Engineering, Beihang University, Beijing, China; E-mail: liuhaoyuan24@buaa.edu.cn

Yu Feng

School of Civil Engineering, Sun Yat-sen University, Zhuhai, China & State Key Laboratory for Tunnel Engineering, Sun Yat-Sen University, Guangzhou, China. E-mail: fengy253@mail.sysu.edu.cn

Abstract

With the advantages of low construction costs and rapid installation, suction caissons are widely used as foundations in offshore engineering. This study investigates the influence of spatial variability in the compression-to-extension strength ratio of soil on the ultimate moment load, ultimate rotation, and failure mechanism of suction caisson foundations in sandy soils under horizontal loading. The upgraded SANISAND-MS model is employed to accurately capture sand behavior. A three-dimensional finite element analysis, combined with random field simulation of soil's spatial variability, simulates the response of laterally loaded suction caissons in spatially varying soils. Results indicate that spatial variability leads to a significant discrepancy between the ultimate load in random and uniform soils. Assuming uniformity in c overestimates the ultimate load and rotation. These findings highlight the importance of incorporating reliability indices in the design process.

Keywords: Offshore foundation; suction caisson, spatial variability, random field, Monte Carlo simulation.

1. Introduction

A suction caisson is an inverted steel caisson foundation used for offshore oil and gas platforms and as an anchor for floating structures (Gao et al., 2021; Randolph & Gourvenec, 2017). Due to the ease of installation and low cost, suction caisson is increasingly used as an alternative to monopiles in offshore wind turbine (OWT) foundations (Cox & Jones, 2011; Houlsby & Byrne, 2000). In marine environments, suction caissons are subjected to cyclic loads from wind, waves, and currents, leading to accumulated displacement over time. The foundation design must ensure sufficient bearing capacity and limit displacement. Natural soils often exhibit significant spatial variability due to the depositional, weathering or other processes experienced in their geological histories (Phoon & Kulhawy, 1999). This variability significantly affects foundation bearing capacity and failure mechanisms (Fenton & Griffiths, 2003; Zhang & Dasaka, 2010; Li et al., 2015). Uncertainties in material properties, measurements, and transformation models further complicate OWT foundation design. Nevertheless, the influence of spatially varying soil properties on suction caissons still remains unclear.

2. Methods

2.1 Finite element model of suction caisson foundation

As shown in Fig. 1(a), a three-dimensional finite element (FE) model of suction caisson foundation is developed using the open-source FE software OpenSees (McKenna, 2011). This study considers a suction caisson foundation designed for an 8 MW offshore wind turbine (Zhu et al., 2013). The suction caisson with a height $L = 10$ m and a diameter $D = 20$ m is fully embedded in the soil, supporting a hollow cylindrical platform of height $(H) = 37.5$ m, inner diameter = 3.8 m and outer diameter = 4 m. To minimize the boundary effects, the dimension of the numerical model is set as $10D \times 5D \times 4L$. The bottom boundary is fixed in all directions, while the lateral surfaces are subjected to only horizontal displacement constraints and the top surface is set free.

The suction caisson and the upper structure are modeled as steel using a linear elastic constitutive model, defined by Young's modulus of $E_{\text{steel}} = 2.21 \times 10^8$ kPa, a Poisson's ratio of $\nu_{\text{steel}} = 0.3$, and a density of

$\rho_{\text{steel}} = 7.85 \text{ g/cm}^3$. The soil is selected to be uniform China ISO standard sand with an initial relative density of 50% and a dry unit weight 16.5 kN/m^3 , and is described using the constitutive model called the upgraded SANISAND-MS model (Lan et al., 2023). The upgraded SANISAND-MS model involves 18 parameters including a monotonic subset ($n \sim n_d$) and a cyclic subset ($\mu_0 \sim \beta$), which are calibrated through triaxial tests listed in Table 1.

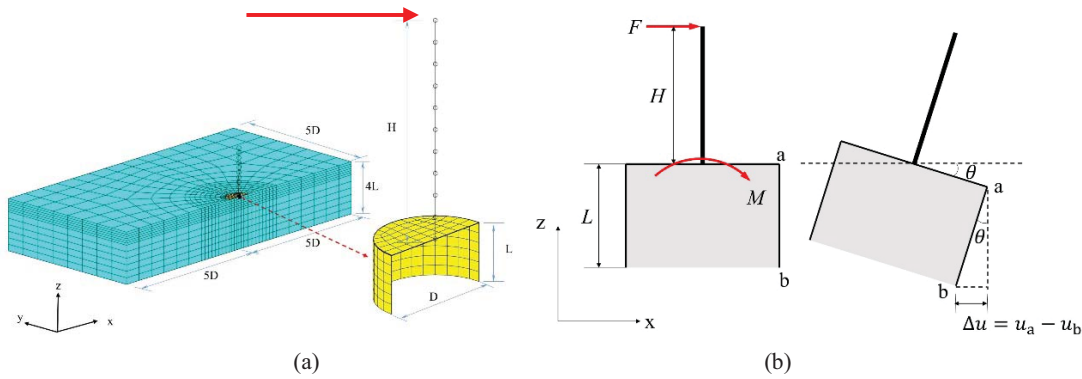


Fig. 1. (a) Schematic diagram of 3D-FE model of soil-suction caisson interaction; (b) definition of moment load and rotation of the suction caisson.

The suction caisson was assumed to be wished-in-place before applying any horizontal load. As illustrated in Fig. 1b, the horizontal load (F) was applied at the top of the upper platform. The moment load (M) at the top surface of the suction caisson is calculated as $M = FH$. The corresponding rotation angle (θ) of the suction caisson is obtained using the formula: $\theta = \arcsin[(u_a - u_b) / L]$, where the u_a and u_b are the horizontal displacements (in x direction) of the reference points on the suction caisson.

Table 1 The parameters of the upgraded SANISAND-MS model for China ISO standard sand

Model features	Parameters	Value
Elasticity	n	0.2
	ν	0.18
	k	400
	γ	0.96
Critical state	M	1.3
	c	0.712
	λ_c	0.016
	e_0	0.589
	ξ	0.7
Yield surface	m	0.01
Plastic modulus	h_0	1.0
	c_h	0.9
	n_b	3.3
Dilatancy	A_0	0.7
	n_d	5.0
Memory surface	μ_0	32
	ζ	0.0018
	β	1

2.2 Random field simulation

Spatial variability is often modeled as a random field characterized by the mean value (μ), coefficient of variation (COV), and autocorrelation distance (ρ) (Vanmarcke, 1977). In this study, for illustrative purpose, only the compression-to-extension strength ratio (c) is modeled as a log-normal random field with a mean value of $\mu_c = 0.17$, COV of 40%, and spatial autocorrelation distance of $\rho_x = 10 \text{ m}$. The autocorrelation distance is assumed to

be the same in both the x and y directions and the horizontal to vertical value ratio is set to $\rho_x/\rho_z=10$. The matrix decomposition method is used in this study. The whole soil domain is divided into 4192 elements on which the random field is to be mapped. The soil properties vary from element to element to reflect the spatial variability of soils. The random field follows a single exponentially decaying autocorrelation function, which provides the values of the correlations between two arbitrary points $X(x, y, z)$ and $X'(x', y', z')$ as given by:

$$\rho = \exp\left(-2\sqrt{\frac{\Delta x^2}{\delta_x^2} + \frac{\Delta y^2}{\delta_y^2} + \frac{\Delta z^2}{\delta_z^2}}\right) \tag{1}$$

where Δx , Δy and Δz denote the distance between any two points of a random field in the space along the x -, y -, and z -direction, respectively; δ_x , δ_y , and δ_z represent the autocorrelation distance in the x -, y -, and z -direction, respectively.

Fig. 2(a) illustrates the evolvement of the autocorrelation matrix, M , in 3D shape analysis (x, y , and z axes). The autocorrelation matrix, M , of the random field is created by computing the autocorrelation coefficients for any two points spaced at any distance and aligned with any direction. The locations where the soil properties are involved in the computation of the correlation distance are considered unit center points. Fig. 2(b) shows a realization of the generated random fields, where red regions indicate the stronger zone with a higher value and the blue regions represent the weaker part.

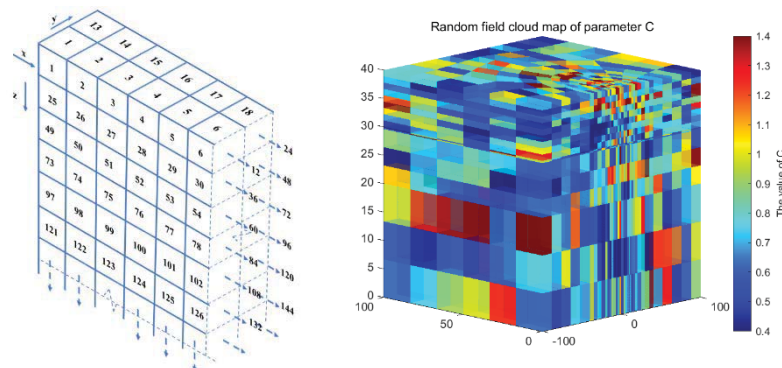
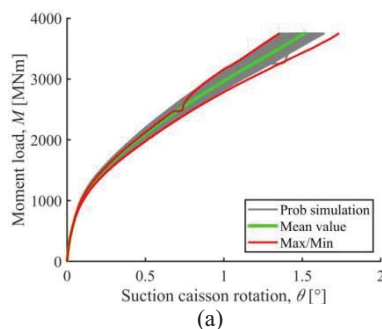


Fig. 2.(a) The sequence of three-dimensional elements in the random filed; (b) One random field realization of compression-to-extension strength ratio

3. Results

Monte Carlo simulations were conducted with 300 realizations. Fig. 3(a) shows the moment-rotation responses, comparing 300 realizations from the Monte Carlo simulation with the results of the deterministic analysis. The ultimate moment load (M_u) was determined using the double tangent intersection criterion (Boushehrian et al. 2009). The M_u and the corresponding rotation of the suction caisson for deterministic analysis were determined as: $M_u = 3039.1$ MN, $\theta_u = 1.83^\circ$. Fig. 3(b) and 3(c) illustrate the volumetric strain distribution for the upper-bound realization and the lower-bound realization. The mobilized soil volume may be influenced by variations in soil conditions, ultimately leading to different M_u . If a realization contains a large volume of weak soil, failure occurs through these weaker zones, resulting in a lower M_u . Conversely, when the pile foundation is surrounded by a significant volume of stiff soil, it provides greater resistance, leading to a higher M_u . Comparing Fig. 3(b) and Fig. 3(c), Fig. 3(b) involves a larger volume of mobilized soil, which contributes to a higher M_u .



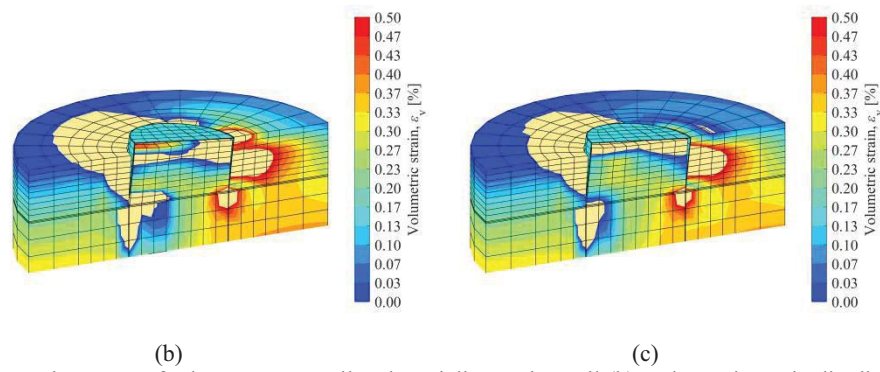


Fig. 3. (a) Moment-rotation curves for homogenous soil and spatially varying soil; (b) Volumetric strain distribution for the upper-bound realization; (c) Volumetric strain distribution for the lower-bound realization.

Fig. 4(a) and 4(b) summarize the results of the empirical probability density function (PDF) for M_u and θ_u . The distribution of the M_u fits well with the normal distribution. Monte Carlo simulations indicate that the mean M_u is approximately 0.2 MNm lower than that of homogeneous soil, while the mean θ_u about 0.9° lower. This pattern indicates that the spatial variability of the soil is likely to reduce the M_u and θ_u of the suction caisson. Results indicate that spatial variability leads to a significant discrepancy between the ultimate load M_u and θ_u in random and uniform soils. Assuming uniformity in c overestimates the ultimate load and rotation. These findings highlight the importance of incorporating reliability indices in the design process.

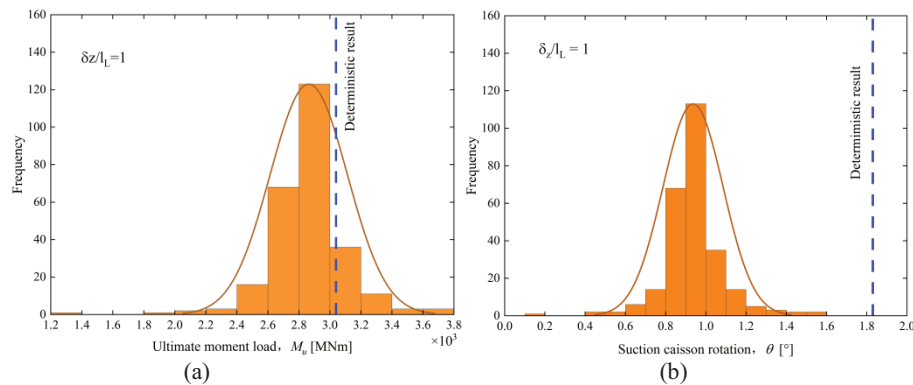


Fig. 4. (a) Histogram estimated normal distribution of M_u and (b) Histogram estimated normal distribution of θ_u

4. Conclusion

This study investigated the impact of soil spatial variability on the performance of suction caissons in sandy soils under horizontal loading. Using the upgraded SANISAND-MS model and a three-dimensional finite element analysis combined with random field theory, the study revealed that spatial variability significantly influences the ultimate moment load, ultimate rotation, and failure mechanisms of suction caissons. Monte Carlo simulations demonstrated that assuming uniform soil properties leads to an overestimation of both ultimate load and rotation. Specifically, the mean ultimate moment load (M_u) and rotation (θ_u) in spatially varied soils were found to be lower than in homogeneous soil conditions, emphasizing the necessity of incorporating soil variability in design considerations. These findings highlight the importance of accounting for uncertainty and reliability indices in offshore foundation design to ensure safer and more efficient structures. Future research could investigate the impact of different parameter random field distributions on the performance of suction caisson foundations and extend the methodology to cyclic loading conditions to analyze its effects on accumulated deformation.

5. Acknowledgements

This work was funded by the National Natural Science Foundation of China (No. 52279121; 52025094), Guangdong Basic and Applied Joint Funding for Offshore Wind Power (No. 2023A1515240069) and Science and Technology Innovation Program from Water Resources of Guangdong Province (2024-05).

References

- Boushehrian, A.H., Hataf, N., Ghahramani, A., (2009). Numerical study of cyclic behavior of shallow foundations on sand reinforced with geogrid and grid-anchor. *IJCEE* 3: 390–393.
- Cox, J. A., O'Loughlin, C. D., Cassidy, M., Bhattacharya, S., Gaudin, C., & Bienen, B. (2014). Centrifuge study on the cyclic performance of caissons in sand. *International Journal of Physical Modelling in Geotechnics*, 14(4), 99-115.
- Fenton, G. A., and Griffiths, D. V. (2003). Bearing Capacity Prediction of Spatially Random c - ϕ Soils. *Canadian Geotechnical Journal*, 40(1), 54-65.
- Gao, B., Ye, G., Zhang, Q., Xie, Y., Yan, B., (2021). Numerical simulation of suction bucket foundation response located in liquefiable sand under earthquakes. *Ocean Engineering*, 235(1): 109394.
- Houlsby, G.T. (2016). Interactions in offshore foundation design. *Geotechnique*, 66(10): 791-825.
- Lan, H., Liu, H.Y., Zhao, H., (2023). Impact of hyper-elasticity on cyclic sand modelling: A numerical study based on SANISAND-MS. *Computers and Geotechnics*, 159: 105428.
- Li, J., Tian, Y. H., and Cassidy, M. J. (2015). Failure mechanism and bearing capacity of footings buried at various depths in spatially random soil. *Journal of Geotechnical and Geoenvironmental Engineering*, 141(2), 01014099.
- Liu, H.Y., Abell, J.A., Diambra, A., and Pisanò, F. (2019). Modelling the cyclic ratcheting of sands through memory-enhanced bounding surface plasticity. *Géotechnique* 69, (9), 783–800.
- Phoon, K. K., and Kulhawy, F. H. (1999). Characterization of geotechnical variability. *Canadian Geotechnical Journal*, 36 (4), 612-624.
- Randolph, M., Gourvenec, S., (2017). *Offshore geotechnical engineering*. London, CRC press.
- Zhang, L. M., and Dasaka, S. M. (2010). Uncertainties in geologic profiles versus variability in pile founding depth. *Journal of geotechnical and geoenvironmental engineering*, 136(11), 1475-1488.